Proc. Asia-Pacific Econophysics Conf. 2016 — Big Data Analysis and Modeling toward Super Smart Society — (APEC-SSS2016)
JPS Conf. Proc. **16**, 011002 (2017)
https://doi.org/10.7566/JPSCP.16.011002

Multi-universality and localized attacks in spatially embedded networks

Bnaya Gross[1*], Dana Vaknin[1*], Michael M. Danziger[1] and Shlomo Havlin[1,2]

[1]*Department of Physics, Bar Ilan University, Ramat Gan, Israel*
[1*] *These authors contributed equally to this work*
[2]*Institute of Innovative Research, Tokyo Institute of Technology, Midori-ku, Yokohama, Japan 226-8503*

E-mail: havlin@ophir.ph.biu.ac.il

(Received October 31, 2016)

We study a realistic spatial network model constructed by randomly linking lattice sites with link-lengths following an exponential distribution with a characteristic scale ζ. We find that this simple spatial network topology does not fulfill any single universality class, but exhibits a new *multi-universality* with two sets of critical exponents. This bi-universality is characterized by random–like scaling laws for measurements on a scale smaller than ζ but spatial scaling for measurements on a larger scale. We further explore this topology by studying the resilience of a two-layer multiplex under localized attack. We find that for a broad range of the control parameters, our system is metastable. In this metastable region, a localized attack larger than a critical size — that does not depends on the size of the system — induces a propagating cascade of failures leading to the system collapse.

KEYWORDS: Percolation Theory, Critical Exponents, Universality Classes, Spatial Networks, Interdependent Networks, Multiplex Networks.

1. Introduction

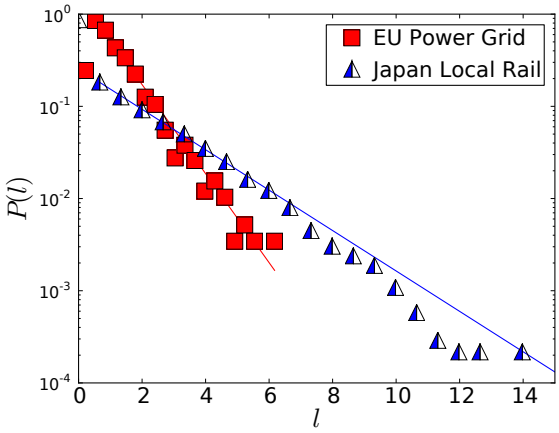

Fig. 1. Examples of real-world networks with links of characteristic length. The link-length distribution of EU Power Grid and the Japan Local Rail, normalized for visibility. The normalized value of the data is 3.7 km (power) and 1.0 km (rail), and the characteristic length is 4.8 km (power) and 1.2 km (rail) if measured as the mean or 3.3 km (power) and 2.0 km (rail) if measured as the inverse slope of the fit. After [1].

When a complex network is embedded in space, it obtains a new property: geometric link length. If the spatial effects are weak, all link-lengths are *a priori* equally likely. However, when the spatial effects are strong, shorter links will be much more likely and it makes sense to model the link-length distribution with a short-tail distribution like the exponential. This assumption is borne out by real-world networks, as shown in Fig. 1. This idea was first suggested by Waxman [2] and later studied for the Ising model embedded in space in annealed complex networks [3, 4].

Complex networks are typically studied as either random or spatial [5–7] with little attention given to the unique universality features of topologies sharing elements of both. Though the well-known small-world model [8, 9] allows simple transitioning from lattice to random, its universality properties become random-like for even very-small rewiring probabilities [10, 11].

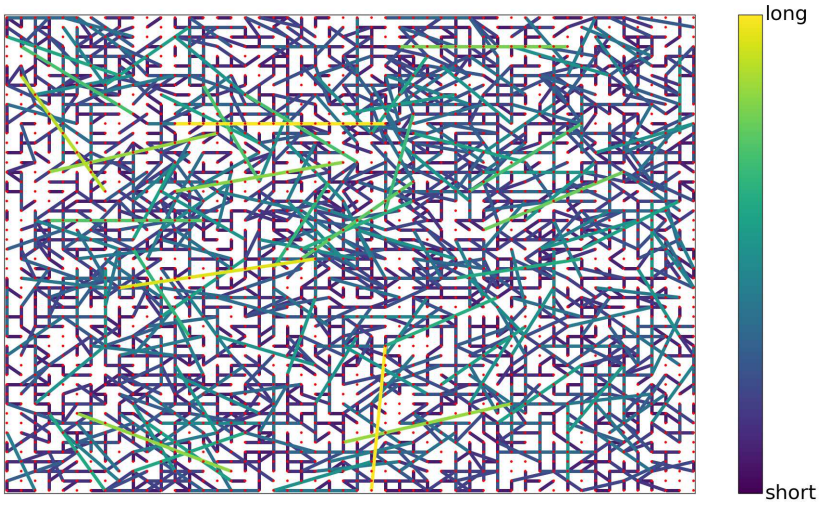

Fig. 2. Demonstration of a network with exponential distribution, Eq. (1)**.** It can be seen that there are many short range edges and only few long range. The network size is 50×50 for $\langle k \rangle = 2$ and $\zeta = 2$.

One of the most powerful findings of statistical physics is the discovery of *universality classes* which can be used to categorize and predict the behavior of seemingly different systems. Various models on lattices have been studied so far in the context of percolation theory and their collective properties have been fully characterized by studying the scaling of various parameters, such as the size of the giant component, the correlation length or the average size of finite clusters. Near criticality, all these quantities scale as power laws of the control parameter of the system. The exponents in these power laws have been shown to be related to each other by means of a set of scaling relations [12].

In addition, in recent years, world-wide human technological, social and economic systems have become more and more integrated and interdependent [13–18]. Therefore, there is a need of modeling these systems as interdependent for understanding their structure, function and robustness [19–26]. Studies on spatially embedded interdependent networks found that in many cases they are significantly more vulnerable then non-embedded systems [27]. Further studies deal with similar models but restrict the dependency links to be of limited length [28–31].

In many cases, a complex network may be subject to damage or attack that is spatially localized such as natural disaster or terrorist attacks. Recent studies show that localized attacks on some systems are significantly more damaging compared to random attacks [32, 33]. A study of localized attacks

on two interdependent lattices with dependency links of limited length, found a metastable region in which a localized attack larger than a critical finite size, induces a cascade of failures which propagate through the whole system leading to its collapse [34].

The combination of spatially constrained connectivity links and multiplex dependency—both ubiquitous features of real complex systems—makes these systems vulnerable to potentially catastrophic localized attacks. These attacks are important and realistic because they can represent local damage on two spatial networks that depend on one another to function in a natural way — the nodes are either the same, or every node in one network layer depends on the closest node in the other. In addition, because of the interdependency between the networks the phase transition is abrupt, the collapse after an attack is sudden and not containable once it starts.

Here we study a recently developed spatial embedded network model, whose aim is to give a better description of real–world space embedded networks and of critical phenomena which takes place in them [1]. We focus on two main aspects of this topology: (*i*) the unique percolation critical behavior in the single-layer case, and (*ii*) the vulnerability to localized attacks in the multiplex case. In both we find unique and surprising properties: multi-universality in the first case and metastability in the second. We will begin by describing the model and then the results for each case.

In this spatial topology, the nodes are distributed as on a square lattice and the links are assigned at random with an exponential link-length distribution:

$$P(r) \sim \exp\left(-r/\zeta\right), \tag{1}$$

as illustrated in Fig. 2. Each link-length has a probability according to Eq. (1) and links which follow this distribution are generated and added at random until the desired $\langle k \rangle$ is obtained. Here ζ is a parameter determining the characteristic link length and thereby the strength of the embedding — the smaller ζ is, the stronger the embedding is. Real network realizations supporting this model are shown in Fig.1 [1]. For the multiplex case, we generate two (or more) sets of links with the same set of nodes. In general there can be a different values of $\langle k \rangle$ and ζ for each layer though for this work, we focus on the two-layer case where they are the same in both.

2. Results

2.1 Universality Classes in a Spatial Network Model

We begin by analyzing the geometric distance as a function of chemical distance between pairs of nodes for percolation at criticality [35]. We denote by $\langle r \rangle$ the average geometric distance at chemical distance l which is the minimal number of hops (number of links) between them. For percolation we denote the parameter p that represents the probability for a single node to be occupied (not removed) in the network and p_c is the critical threshold above which a giant component emerges. The algorithm to measure $\langle r \rangle$ is as follows: (*i*) randomly select a single node from the giant component at criticality to be a source node, (*ii*) measure the geometric distances from this source to all nodes l steps away (chemical distance l) from the source, (*iii*) average all the geometric distances obtained in step (*ii*). Repeat this process over all the nodes in the giant component, and average over all sources. We find that our network behaves for scales smaller than ζ differently compared to scales larger than ζ,

$$\langle r \rangle = \begin{cases} l^{1/2} & l \leq l^* \\ l^{1/1.13} & l > l^* \end{cases} . \tag{2}$$

To understand the origin of the two regions of critical exponents we note that for $r < \zeta$ the structure of the lattice is not relevant since every pair of nodes can be connected with almost the same probability, as per Eq. (1). This results in a mean-field-like behavior because the space is irrelevant, similar to $d \geq 6$ [1]. However, for $r > \zeta$ the links are much shorter than the measurement scale and the underlying two-dimensional lattice structure determines the behavior. Thus, these two exponents $1/2$ and $1/1.13$

are expected since they have been found for percolation in $d \geq 6$ (MF) and for $d = 2$ respectively [35]. In $d \geq 6$ the spatial restrictions are irrelevant and the path is like a random walk ($\langle r^2 \rangle \sim t$ (number of steps)). To derive Eq. (2) from a single scaling function, we propose the scaling ansatz,

$$\langle r \rangle = \zeta l^{1/2} f\left(\frac{l}{l^*}\right) \tag{3}$$

where,

$$f(x) = \begin{cases} const & x \leq 1 \\ x^{\alpha} & x > 1 \end{cases} . \tag{4}$$

Here, l^* is assumed to scale as $\zeta^{1.13}$. Indeed, from the scaling function Eq. (3), by using Eq. (4) and identifying $\alpha = 1/1.13 - 1/2$, we obtain Eq. (2). Our scaling assumption, Eq. (3), is supported by simulations shown in Fig. 3.

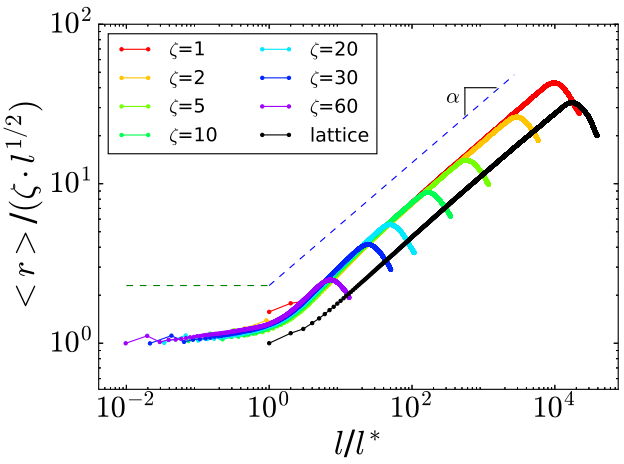

Fig. 3. The average geometric distance $\langle r \rangle$ as a function of the chemical distance l at criticality. Both y-axis and x-axis scale according Eq. (3). Averages are taken over more then 200 realizations where each network has 10^8 nodes. The scaling relation is : $r = \zeta l^{1/2} f\left(\frac{l}{l^*}\right)$ where $l^* = \zeta^{1.13}$. It can be seen that after the scaling, the graph starts as nearly constant for $\frac{l}{l^*} \ll 1$ and then crosses over at $l \sim l^*$ to a slope with exponent α. Note that for the pure lattice the constant region does not exist and as ζ increases the constant region gets longer and the region with the exponent of α gets shorter. The bending down of the curves are due to finite size of the systems. For infinite systems the bending down will disappear.

Next, we ask whether the bi-universality phenomena is unique for percolation at criticality or whether it is general and can be observed also not at criticality. Hence we calculate directly the geometric distance as a function of chemical distance and the network dimension when the network is full i.e., $p = 1$. The algorithm to measure the geometric distance as a function of chemical distance when the network is full is the same as described above for criticality. Simulation results are shown in Fig. 4. It is seen that for small l the distance r behave approximately as $r \sim l^{1/2}$ while for large l, $r \sim l$. Indeed, we expect that the behavior of the network will follow:

$$\langle r \rangle = \begin{cases} l^{1/2} & l \leq l^{**} \\ l & l > l^{**}. \end{cases} \tag{5}$$

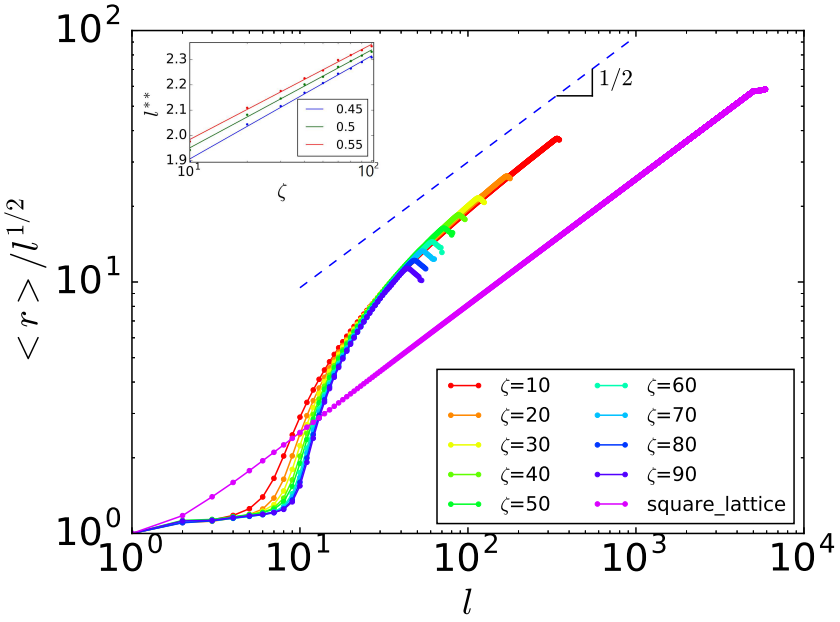

Fig. 4. The average geometric distance $\langle r \rangle$ as a function of the chemical distance l when the network is full ($p = 1$)**.** Average over more then 200 realizations are taken and the network has 10^8 nodes. The scaling relation shown: $r = l^{1/2} f(x)$. Here one can see that after scaling the graph behavior starts approximately as a constant and then crosses over to exponent of $1/2$. For lattice the constant region does not exist and as ζ increases the constant region gets longer. The inset demonstrates the logarithmic scaling of l^{**} with ζ. The inset shows the crossover point l^{**} as a function of ζ for different values of $\langle r \rangle / l^{1/2}$ above the constant region.

This is because at short distances we expect a random behavior and at large distances we expect spatial behavior. The crossover l^{**} is expected to occur at $l^{**} \sim log(\zeta^2)$ since for mean field (or ER) the shortest path behaves as $l \sim logN \sim log(\pi \cdot r^2)$. Support for this relation is presented in the inset of Fig. 4. To derive Eq. (5) from a single scaling function, we propose,

$$\langle r \rangle = l^{1/2} f(x) \tag{6}$$

where,

$$f(x) = \begin{cases} constant & x \leq l^{**} \\ l^{1/2} & x > l^{**}. \end{cases} \tag{7}$$

Note that Fig. 4 is plotted after scaling using Eq. (6) and Eq. (7). In this figure, the graph start as constant and then crossover to the exponent $1/2$. As can be seen, as ζ increases the crossover emerges later where for lattice there is no constant behavior, see inset of Fig. 4 for the scaling of the crossover.

We also evaluated the network dimension directly following the method of Li et al [36]. To this end we first measured $\langle r \rangle$ as a function of l as shown in Fig. 4, and then we calculated the mass (number of sites), M, as a function of l. Using both measurements we can plot M vs r whose exponent determines the dimension d of the system [36]. The results are demonstrated in Fig. 5, where the slope (power-law exponent) shows the network dimension. One can see that at short scale the slope approach infinite i.e., the dimension is diverging (see the inset of Fig. 5) and at large scale the slope approaches 2 indicating that the dimension of the network is 2 as expected for the $d = 2$ spatial network. As ζ increases the crossover emerges at larger l and the slope of the random region tends to infinity as can be seen in the inset of Fig. 5.

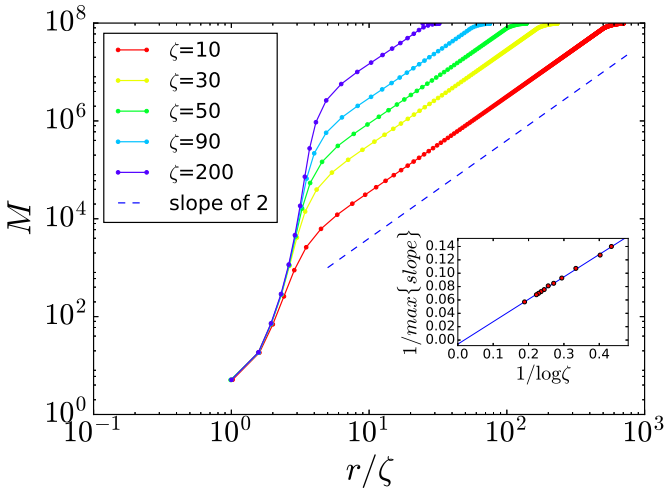

Fig. 5. The dimension of the system when the network is at $p = 1$. Average is taken over more then 100 simulations and the network has 10^8 nodes. Here one can see that at short scales the slope is diverging as can be shown from the inset and then a crossover emerges with a slope of 2.

In conclusion, we see that our model network exhibits two types of scaling behavior due to the exponential distribution link-length topology. For short scales ($r < \zeta$) it behaves like an infinite dimensional system with mean-field exponents, while for longer scales ($r > \zeta$) the two-dimensional exponents are observed.

2.2 Localized Attacks on Spatial Multiplexes

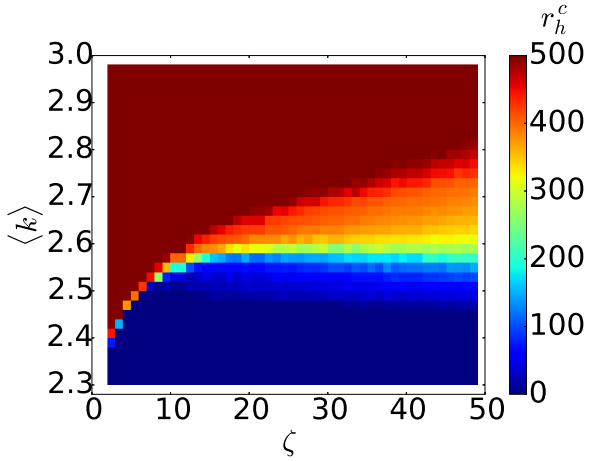

Fig. 6. Phase diagram of the critical attack size r_h^c. Dependence of the critical attack size r_h^c on the average degree $\langle k \rangle$ and the characteristic link length ζ. The color bar on the right represents the size of r_h^c in lattice units. In this figure the network size is 1000×1000, with averages over 20 runs are taken for each data point.

Real-world networks rarely appear in isolation. For example the power grid and communication

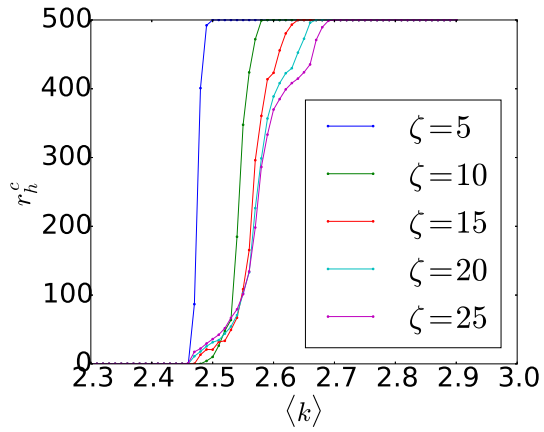

Fig. 7. The critical attack size r_h^c as a function of average degree $\langle k \rangle$. The figure demonstrates the critical radius along vertical lines in Fig. 6. As expected, the system is more stable for larger $\langle k \rangle$, yielding larger r_h^c. In this figure the network size is 1000×1000, with averages over 20 realizations for each data point.

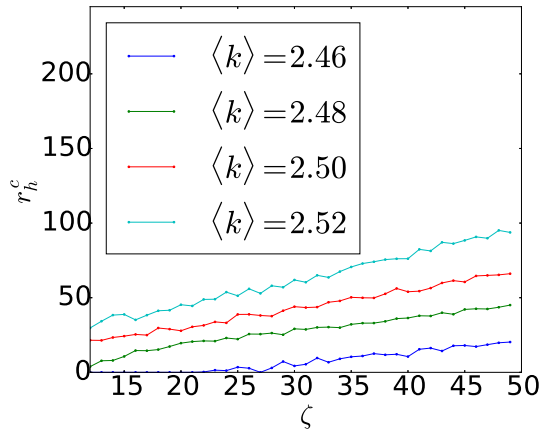

Fig. 8. The critical attack size r_h^c as a function of ζ at the metastable region. This figure represents horizontal lines in Fig. 6. The critical radius r_h^c increases almost linearly as a function of ζ. In this figure the network size is 1000×1000 and averages over 20 runs are taken for each data point.

system depend on one another [18]. Therefore, it is important to understand the spatial network topology discussed above in the case of interacting networks. Though random failures in multiplex networks of this topology have been studied [1], localized attacks—which occur frequently in real world due to natural disasters or terrorist attacks—have not been studied on multiplex embedded structures.

In this section, we describe our study of the resilience of a multiplex under localized attack. For simplicity, we focus on the case in which the 2-d lattice layers have the same characteristic link length ζ and same average degree $\langle k \rangle$ as described above. The multiplex network with two layers is equivalent to two interdependent networks if the dependency links have length zero, while the connectivity links are random but restricted by the link-length distribution in Eq. (1).

For a node to remain functional in our model it must be connected to the giant component in

both layers, reflecting, for example, the need for electricity and communication connectivity of a neighborhood or communications station. Therefore, we perform a localized attack on the two layers multiplex, as follows: (*i*) We remove all nodes within a distance r_h from a random location in the system. (*ii*) From the set of the remaining nodes, we remove all the nodes that are not in the giant component of the first layer. (*iii*) We repeat step (*ii*) in the second layer. (*ii*) and (*iii*) are repeated until there are no nodes to remove, in other words, we have the mutual giant component (MGC) of the two layers in the multiplex.

At the end of this cascade, the system is categorized as functional or non-functional depending on whether the MGC, the largest set of nodes that are connected in both layers, is of the order of the system size or not. This reflects the assumption that nodes must be connected in both layers in order that the multilayer system will be functional. For example, in a multilayer system of electricity and its controlled communication network large component of nodes in both layers must be connected in order that the multilayer system will be functional.

We analyzed the effects of the localized attack on the multiplex for different $\langle k \rangle$, ζ and r_h. Our simulations suggest the existence of r_h^c, the minimum radius needed to cause the system to collapse. When we calculate the critical attack radius r_h^c for different $\langle k \rangle$ and ζ, we discover three regions, as shown in the phase diagram in Fig.6. The regions are: (*i*) Stable (in dark red) — in this region the system remains functional after localized attack of any finite size. (*ii*) Unstable (in blue) — in this region the system is non-functional even if no nodes are removed. (*iii*) Metastable (between the above-mentioned regions) — in this region only attacks with radius larger than r_h^c yield breakdown where the system becomes fully non-functional. As expected and observed in Fig.7, the system is more stable for larger $\langle k \rangle$, i.e., r_h^c sharply increases. Additionally, as seen in Fig.8, at the metastable region, we find that r_h^c increases almost linearly as a function of ζ.

3. Discussion

Here, we have analyzed a simple spatial topology based on modifying the link-length distribution on an underlying grid spacing of nodes, following [1]. We find that in single layers, this topology displays fascinating multi-universality: for measurements of length below ζ, the network exhibits random scaling behavior, while for measurements of longer lengths, it appears as a lattice-like. This sheds new light on real-world systems which may not appear to fit any single universality class. It is possible that real systems are in fact in multiple classes, depending on the scale of the measurement. Empirical measurements of real-world networks suggests that this may be the case (cf. Fig. 1) but available data sets lack spatial homogeneity on a wide enough scale to verify this directly. We further probe this topology by considering its response to localized attacks in a multiplex. This combination of features (characteristic link-length topologies, interdependence between layers and localized failures/attacks) is ubiquitous yet largely ignored. We find that it exhibits metastability for a wide range of system parameters, where small and finite size localized damage can spread and destroy the entire system.

Acknowledgement

The authors acknowledge the MULTIPLEX (No. 317532) EU project, the Israel Science Foundation, Israel Ministry of Science and Technology (MOST) with the Italy Ministry of Foreign Affairs, MOST with the Japan Science and Technology Agency, BSF-NSF Grant Number 2015781, ONR and DTRA for financial support. MMD thanks the Azrieli Foundation for the award of an Azrieli Fellowship grant.

References

[1] M. M. Danziger, L. M. Shekhtman, Y. Berezin, and S. Havlin: EPL (Europhysics Letters) **115** (2016) 36002.
[2] B. Waxman: Selected Areas in Communications, IEEE Journal on **6** (1988) 1617.
[3] S. Bradde, F. Caccioli, L. Dall'Asta, and G. Bianconi: Phys. Rev. Lett. **104** (2010) 218701.
[4] A. Halu, S. Mukherjee, and G. Bianconi: Phys. Rev. E **89** (2014) 012806.
[5] M. Barthélémy: Physics Reports **499** (2011) 1 .
[6] B. Bollobás: *Random Graphs* (Cambridge University Press, 2001) second ed.
[7] M. Newman: *Networks: an introduction* (OUP Oxford, 2010).
[8] D. J. Watts and S. H. Strogatz: Nature **393** (1998) 440.
[9] M. Barthélémy and L. A. N. Amaral: Physical Review Letters **82** (1999) 3180.
[10] M. E. J. Newman and D. J. Watts: Phys. Rev. E **60** (1999) 7332.
[11] M. E. J. Newman, I. Jensen, and R. M. Ziff: Phys. Rev. E **65** (2002) 021904.
[12] H. Stanley: *Introduction to Phase Transitions and Critical Phenomena* (International series of monographs on physics. Oxford University Press, 1971), International series of monographs on physics.
[13] R. Bookstaber and D. Y. Kenett: OFR Brief **16** (2016).
[14] A. Majdandzic, L. A. Braunstein, C. Curme, I. Vodenska, S. Levy-Carciente, H. E. Stanley, and S. Havlin: Nature communications **7** (2016).
[15] W. Li, D. Y. Kenett, K. Yamasaki, H. E. Stanley, and S. Havlin: ArXiv e-prints (2014).
[16] J. Peerenboom, R. Fischer, and R. Whitfield: Proc. CRIS/DRM/IIIT/NSF Workshop Mitigat. Vulnerab. Crit. Infrastruct. Catastr. Failures, 2001.
[17] S. Rinaldi, J. Peerenboom, and T. Kelly: Control Systems, IEEE **21** (2001) 11.
[18] V. Rosato, L. Issacharoff, F. Tiriticco, S. Meloni, S. D. Porcellinis, and R. Setola: International Journal of Critical Infrastructures **4** (2008) 63.
[19] S. V. Buldyrev, R. Parshani, G. Paul, H. E. Stanley, and S. Havlin: Nature **464** (2010) 1025.
[20] J. Gao, S. V. Buldyrev, H. E. Stanley, and S. Havlin: Nature Physics **8** (2012) 40.
[21] J. Gao, S. V. Buldyrev, S. Havlin, and H. E. Stanley: Phys. Rev. Lett. **107** (2011) 195701.
[22] G. J. Baxter, S. N. Dorogovtsev, A. V. Goltsev, and J. F. F. Mendes: Phys. Rev. Lett. **109** (2012) 248701.
[23] M. Kivelä, A. Arenas, M. Barthélémy, J. P. Gleeson, Y. Moreno, and M. A. Porter: Journal of Complex Networks **2** (2014) 203.
[24] M. De Domenico, A. Solé-Ribalta, E. Cozzo, M. Kivelä, Y. Moreno, M. A. Porter, S. Gómez, and A. Arenas: Phys. Rev. X **3** (2013) 041022.
[25] S. Boccaletti, G. Bianconi, R. Criado, C. Del Genio, J. Gómez-Gardeñes, M. Romance, I. Sendina-Nadal, Z. Wang, and M. Zanin: Physics Reports (2014).
[26] G. Bianconi: Phys. Rev. E **87** (2013) 062806.
[27] A. Bashan, Y. Berezin, S. V. Buldyrev, and S. Havlin: Nature Physics **9** (2013) 667.
[28] W. Li, A. Bashan, S. V. Buldyrev, H. E. Stanley, and S. Havlin: Phys. Rev. Lett. **108** (2012) 228702.
[29] M. M. Danziger, A. Bashan, Y. Berezin, and S. Havlin: Journal of Complex Networks **2** (2014) 460.
[30] M. M. Danziger, A. Bashan, Y. Berezin, and S. Havlin: Signal-Image Technology Internet-Based Systems (SITIS), 2013 International Conference on, Dec 2013, pp. 619–625.
[31] L. M. Shekhtman, Y. Berezin, M. M. Danziger, and S. Havlin: Phys. Rev. E **90** (2014) 012809.
[32] S. Shao, X. Huang, H. E. Stanley, and S. Havlin: New Journal of Physics **17** (2015) 023049.
[33] X. Yuan, S. Shao, H. E. Stanley, and S. Havlin: Phys. Rev. E **92** (2015) 032122.
[34] Y. Berezin, A. Bashan, M. M. Danziger, D. Li, and S. Havlin: Scientific Reports **5** (2015).
[35] A. Bunde and S. Havlin: *Fractals and disordered systems* (Springer-Verlag New York, Inc., 1991).
[36] D. Li, K. Kosmidis, A. Bunde, and S. Havlin: Nature Physics **7** (2011) 481.